JOURNAL OF COAL SCIENCE & ENGINEERING
(CHINA) DOI 10.1007/s12404-011-0311-1
pp 285–289 Vol.17 No.3 Sep. 2011

DPM dissipation experiment at MST's experimental mine and comparison with CFD simulation

ZHENG Yi, LAN Hai, THIRUVENGADAM Magesh, TIEN Jerry C

Department of Mining & Nuclear Engineering, Missouri University of Science and Technology (MST), Rolla MO 65401, USA

Abstract Diesel Particulate Matter (DPM) is regulated in the U.S. for both underground coal and metal/nonmetal mines. Today, many underground mines still face difficulty in compliance with DPM regulations. The DPM research carried out in Missouri University of Science and Technology (MST) is to use computational fluid dynamics (CFD) to study the DPM distribution in commonly used face areas. The result is expected to be used for selection of DPM reduction strategies and better working practices, which can help the underground mines to meet regulation limits and improve the working environment for the miners. An experiment was conducted at MST's Experimental Mine to validate CFD simulation. DPM was collected at four locations downstream of a stationary diesel engine. The experiment data were then compared with the CFD simulation results. The comparison shows that CFD simulation can forecast the location of DPM concentration with practical accuracy (less than 0.15 m). CFD can be used to further study DPM distribution in commonly used working faces and give guidance to DPM reduction.

Keywords DPM, DPM dissipation, CFD, validation study

Introduction

Diesel Particulate Matter (DPM) is a natural by-product from diesel engine operation. With more than a thousand components found in DPM, their adverse health effects have become a great concern. These health effects include acute sensory irritations and respiratory symptoms; premature death from cardiovascular, cardiopulmonary, or respiratory causes and lung cancer (Kahn and Orris, 1988; Anon., 1988, 2002; Wade and Newman, 1993; Rundell et al., 1996).

As a result, the U.S. Mine Safety and Health Administration (MSHA) set a final DPM standard for underground mines on January 19, 2001. For underground metal/nonmetal (M/NM) mines, the final DPM limit of 160 micrograms of total carbon (TC) per cubic meter of air (160 $\mu g/m^3$) became effective on May 20, 2008; for underground coal mines, MSHA required permissible equipment, non-permissible heavy duty equipment, generators, and compressors must emit no more than 2.5 g/h of DPM; non-permissible light-duty equipment must emit no more than 5.0 g/h of DPM. The final rule for underground coal mine became effective on July 19, 2002.

But on the mining side, many companies still face difficulties in compliance with the regulation. According to MSHA compliance data, up to 64% of the personal samples collected in underground M/NM mines still exceed the regulatory limit in its survey from all available mines during the 2003 — 2006 periods (Anon., 2006).

To thoroughly resolve DPM problems, it is critical that DPM propagation characteristics be understood in order to arrive at a sensible and practical method to prevent DPM-related issues through engine maintenance, better ventilation practice, personal protective measures and/or administrative means to be in compliance with regulatory requirements. To achieve this, the computational fluid dynamics (CFD) modeling is used in Missouri University of Science and Technology (MST) to simulate the DPM dissipation and predict their concentration distribution to determine control strategies.

However, comprehensive validation process of CFD modeling against actual mining experiments is an important issue in the application of the CFD results in DPM propagation study. To validate DPM simulation,

Received: 30 March 2011
E-mail:tien@mst.edu

industry field studies have been reconstructed in ANSYS Fluent, a general purpose CFD program, to get the DPM distribution pattern (Zheng and Tien, 2009a and b). One disadvantage of these field studies are that they only provided one set of data at one location. For validation purpose and to know DPM distribution characters, data at multiple locations are more desirable.

This paper shows the validation experiment executed at MST's Experiment Mine. DPM concentration was sampled at four locations downstream of a diesel loader and compared with CFD simulation.

1 Experiment at MST's experimental mine

The aim of the experiment is to measure the DPM concentration at different location downstream of the diesel engine. The data collected in the experiment will be used to validate the simulation results, where CFD method is used to predict the DPM concentration and propagation in the underground mining environment. This validation process will help to transfer CFD expertise to analyze and design the ventilation systems for mines that face difficulties with the DPM regulation.

Fig.1 shows the MST's experimental mine. This mine is located about 2 km from the campus and used solely for education purpose. It is an underground limestone mine using room and pillar mining method and the mine is ventilated from a single airshaft with a JOY series 1000 axial-flow fan, which has the capacity to deliver 17.9 m^3/s of fresh air from the surface. The shaded area in Fig.1 shows the location of the test zone in the mine. Due to the small size of the entry, a 29.8 kW Bobcat loader 753 is used in the experiment. This diesel engine will be operated at a fixed location and fixed operating condition in the test areas and will be the single DPM source in the experiment.

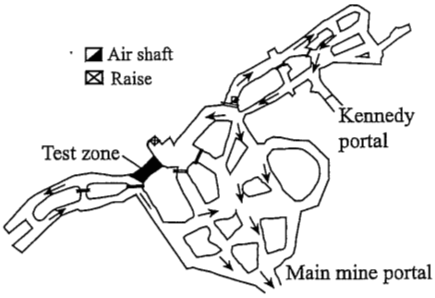

Fig.1 Test zone at MST's experimental mine

The major procedures of this validation study include: experimental design, DPM collection at the mine, DPM deposit analysis from commercial laboratory, experiment simulation through CFD program (ANSYS Fluent) and comparison of simulation and experiment. This paper introduces the DPM collection at MST's experimental mine, describes in detail the CFD model development and is focused on the validation of CFD simulation.

DPM collection in the experiment included five two-hour tests (Test 1~5). In each two-hour test, four samplers (with SKC DPM cassettes) were used to collect DPM. Totally, 20 DPM samples were collected. Fig.2 to Fig.4 shows the experiment layout and the installation of DPM samplers. Before the experiment, the location of the sampling points was measured. It includes measuring the distance of samplers from the tailpipe, the cross section of entry that hangs the sampler and the samplers' exact position in the cross section. Put the engine throttle at a fixed position and mark it. It should not change during all the tests.

Fig.2 Layout of the experiment

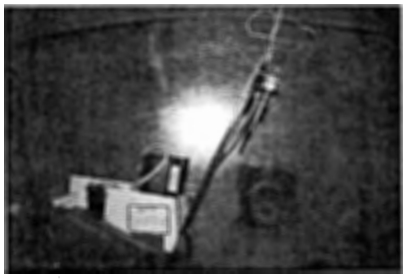

Fig.3 Installation of sampler close to the tailpipe

Fig.4 Installation of sampler from the roof of the entry

2 Development of CFD model

The portion of the test zone shown in Fig.1 is reconstructed for the present computational study as shown in Fig.5. Fresh air flows from the right, sweep through the Bobcat loader and sampling points (P_1, P_2, P_3 and P_4 as in Fig.5). Then flow out of the domain at the left side of the entry as exhaust flow. The height and width are 2.66 m and 2.33 m respectively at the

inlet and outlet of the entry, but the height become inconstant at the sampling areas according to the geometry measured in the mine. The sampler P_1 is pointing toward and set as close (0.33 m) to the tailpipe as possible to calibrate DPM production rate from the exhaust flow. Other positions of samplers are listed in the table below.

Sampler	Distance downstream of tailpipe (m)	Height from the floor (m)	Distance to the right rib (m)
P_2	1.14	1.98	1.00
P_3	3.05	1.66	1.25
P_4	4.52	1.75	1.37

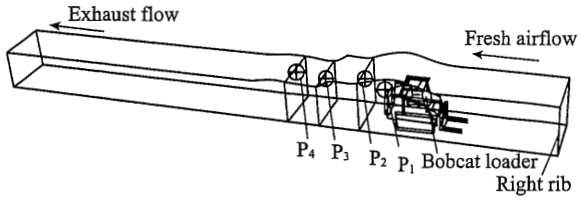

Fig.5 Schematic of the test zone

The computational domain is meshed using ANSYS Fluent's preprocessor GAMBIT as shown in Fig.6. The mesh generation is made by ensuring high density near the Bobcat loader and in the sampling region where high gradients exist, in order to ensure the accuracy of the simulation. Both hexahedral and tetrahedral meshes were generated inside the computational domain as shown in the Fig.6. During mesh generation, the equal-size skewness is monitored and maintained at a value less than 0.8.

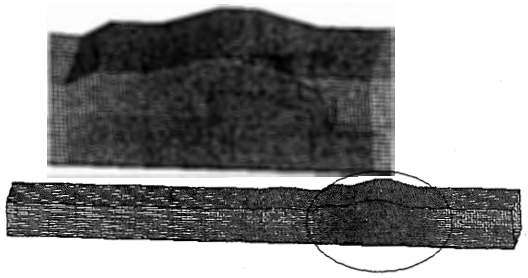

Fig.6 Mesh generation for the computational domain

For this simulation, the physical properties of fresh air flow are treated as constants and evaluated for inlet temperature of T_0=17 ℃ (i.e., specific heat (C_p) is 1 006 J/(Kg • ℃), dynamic viscosity (μ) is 1.789×10^{-5} kg/(m • s), and thermal conductivity (k) equals to 0.024 2 W/(m • ℃). The density variation in the fluid due to temperature gradient that exists between the air intake temperature and the tailpipe emission temperature is calculated using incompressible ideal gas model available in ANSYS Fluent. In this model the flow is assumed to be incompressible but density change due to temperature is calculated using ideal gas law. In the presence of gravity, this density gradient results in buoyancy flow. Numerical simulation of DPM distribution inside the test zone is performed using species transport model available in ANSYS Fluent.

In the species transport model DPM is treated as gas (continuous phase) and the material that is selected as a representative for the DPM is *n*-octane vapor (C_8H_{18}) with density (ρ=4.84 kg/m^3), specific heat (C_p=2 467 J/(Kg •℃)), thermal conductivity (k=0.017 8 W/(m •℃)) and dynamic viscosity ($\mu=6.75\times10^{-5}$ kg/(m • s)). In the species transport model the two species, air and DPM, can diffuse and form a mixture. The mixture properties are derived using incompressible ideal gas law for density, mixing law for specific heat, thermal conductivity and viscosity. The mass diffusivity between air and DPM is assumed to be constant with $D=5\times10^{-6}$ m^2/s. The chemical reaction between the species is not considered in this study.

From the dimensions at the inlet, the hydraulic diameter ($D_h=4A/P$), where A is the inlet cross-sectional area and P the perimeter, is calculated as D_h=2.48 m. The Reynolds number calculated based on this hydraulic diameter is $Re=1.33\times10^5$ and the flow at this Reynolds number is turbulent. The turbulence in the flow is modeled using standard k-ε turbulence model with standard wall functions for near wall treatment.

Other boundary condition used in the simulation include: fresh airflow speed is 0.78 m/s from the entry inlet; exit is set as outflow condition; wall is simulated as no slip boundary and adiabatic wall condition with airflow velocity on the walls as zero. For the tailpipe, the temperature is 127.0 ℃; velocity is 14.4 m/s. The mass fraction for DPM is set at the tailpipe by iteration to make the simulated DPM concentration at P_1 is the same as the experiment data. This way, the model is calibrated by the experiment data at P_1 and validated by comparing DPM concentration at the other sampling points (P_2, P_3 and P_4). For the five two-hour tests (Test 1~5) in the mine, DPM concentration at P_1 for Test 2 is far less than the others and considered as abnormal. Therefore the data for Test 2 are abandoned. For the rest tests, the mass fractions for DPM set at the tailpipe are: 7.201×10^{-6} in Test 1; 5.538×10^{-6} in Test 3; 6.284×10^{-6} in Test 4 and 5.546×10^{-6} in Test 5. Although every aspect is considered to be set as constant during the tests, still DPM production rate from the diesel engine can be variant. To compensate this, every test has to be simulated separately instead of using the average.

Numerical solution of the governing equations and boundary conditions are performed by utilizing the commercial computational fluid dynamics (CFD) code ANSYS Fluent 12.0. The SIMPLE algorithm is used for the pressure velocity coupling, and the momentum, scalar turbulence equations, energy equation and spe-

cies transport equations are discretized using the second order upwind scheme in order to improve the accuracy of the simulations. Second order discretization scheme is used for the pressure equation. Green-Gauss node based method is used to compute gradients in the governing equations. Detailed descriptions of the CFD code and the solution procedures may be found in the ANSYS Fluent 12.0 documentation (Anon., 2009).

3 Comparison of experiment with simulation

Steady simulations are carried out to predict DPM distributions in the test zone that is presented in Fig.5 using ANSYS Fluent CFD code. At least 10 000 iterations were executed for each test simulation to make sure DPM dissipation is steady and well distributed.

The general flow features in the test zone obtained assuming DPM as a different gas (C_8H_{18}) is shown in Fig.7, using contours of DPM colored in the region above the regulation limit (160 μg/m^3). The emissions from the tailpipe start flowing towards the roof of the mine due to the buoyancy force caused by the density difference which in turn is caused by the temperature difference between the fresh intake air and tailpipe emissions forming a turbulent buoyant plume.

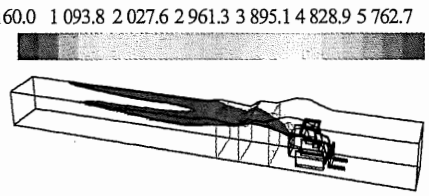

Fig.7 DPM distribution inside the test zone above 160 μg/m^3

The DPM concentration at the four sampling points is shown in Table 1 by comparing the simulation data with experiment data and the difference. The comparison at sampling point 1 (P_1) is very accurate (less than ±0.5%) between the experiment and simulation. That is because DPM sampler at P_1 is the closest one to the tailpipe and its location can be measured with reliable accuracy. Therefore, the experiment data at P_1 are chosen to calibrate the CFD model: first, a random number of less than 10×10^{-6} for the mass fraction of DPM is set at the tailpipe according to previous studies (Zheng and Tien, 2009a and b) to start the simulation. Then DPM concentration is compared at P_1. By trial and error, the simulation will change the mass fraction of DPM at tailpipe to make DPM concentration at P_1 as close to the experiment data as possible.

But the comparison at sampling point 2 to 4 (P_2 to P_4) shows noticeable difference (as high as 56.5% difference) from engineer point of view (which 15% difference may be acceptable). The main reasons causing this difference can be: ① High DPM concentration gradient at the sampling points, therefore within short distance DPM level can change dramatically. ② The location of sampling points is hard to be accurately located in the real mine condition. Although great care is carried out when took the measurement, it is still possible the accuracy is above 5 cm.

Table 1 Comparison of simulation with experiment at sampling points

Test	Sampling	Experiment data(μg/m^3)	Simulation data(μg/m^3)	Difference (%)
1	P_1	2 818.6	2 815.2	−0.1
	P_2	500.0	782.7	56.5
	P_3	323.0	229.5	−28.9
	P_4	247.5	199.4	−19.4
3	P_1	2 161.8	2 166.5	0.2
	P_2	460.8	609.0	32.2
	P_3	222.1	174.7	−21.3
	P_4	204.9	152.0	−25.8
4	P_1	2 436.3	2 424.6	−0.5
	P_2	449.5	525.4	16.9
	P_3	216.2	220.7	2.1
	P_4	209.8	190.7	−9.1
5	P_1	2 161.8	2 161.7	0
	P_2	451.5	550.4	21.9
	P_3	223.5	185.7	−16.9
	P_4	200.0	160.6	−19.7

And the reasoning above provides a clue to look at the results from another angle. Instead of comparing the difference of DPM level between simulation and experiment at the sampling points, the distance of CFD predicted concentration from the experiment data should be examined. Those are shown in Fig.8 for the cross sections of the entry that contain sampling point 2~4. For example, in Fig.8, the simulation DPM concentration at P_2 is shown as 550.4 μg/m^3 (Test 5). P_2 is located at the inner circle of the colored region. However, at P_2, experiment data is 451.5 μg/m^3, which in the simulation domain, this DPM level is located at the outer circle of the colored area. The average width of the colored ribbon can be considered as the accuracy of the simulation and the width for all the data are listed in Table 2. From the table, the maximum distance is 15 cm between the predicted and experiment data at the sampling point (average distance is 10.1 cm at sampling point 4, which is 4.52 m downstream of

the tailpipe). That is to say, if CFD simulation predicts DPM plume to be located in a certain region, the actual DPM level can be ≤15 cm outside or inside the predicted plume. To be on the safe side, 15 cm outside the predicted DPM plume above regulation limit should be considered for the underground mining operations to select working practice and other controlling strategies. CFD simulation at this accuracy can be considered as practically accurate for the mining industry.

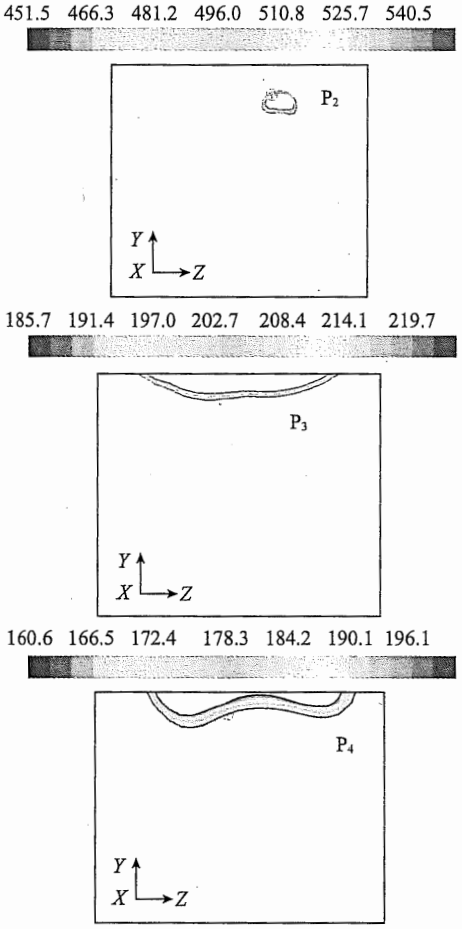

Fig.8 DPM levels between simulation and experiment

Table 2 Average distance of DPM level between simulation and experiment

Sampling	Average distance (cm)			
	Test 1	Test 3	Test 4	Test 5
P_2	6.4	4.8	1.9	2.9
P_3	9.8	7.4	1.0	5.9
P_4	9.6	15.0	5.1	10.6

4 Conclusions

Experiment on DPM dissipation at MST's experimental mine is introduced and CFD simulation is used to reconstruct the experiment to compare the simulation with the experiment. This validation process will help to transfer CFD expertise to analyze and design the ventilation systems for mines that face difficulties with the DPM regulation.

The comparison shows that CFD simulation can forecast the location of DPM concentration with practical accuracy (less than 0.15 m). CFD can be reasonably used to study DPM distribution in commonly used working faces and give guidance to DPM reduction.

Future DPM study includes further validation study by adding more sampling points and simulation of DPM dissipation in straight entry and deadend entry faces. For the validation study, another experiment at MST's Experiment Mine with 27 sampling points downstream of the diesel engine has been finished and waiting for the data to be simulated and compared. For the DPM dissipation study in the face areas, CFD simulation is used to evaluate the effects of mining operations, slope of the face floor, auxiliary ventilation facilities and diesel vehicles motion on the DPM dissipation to provide ready-to-use techniques for the mining industry to comply with the regulation and improve the mining environment for the miners.

References

Anon., 1988. Carcinogenic effects of exposure to diesel exhaust. National Institute for Occupational Safety and Health (NIOSH), Department of Health and Human Services, Publication (No.88-116).

Anon., 2002. Health assessment document for diesel exhaust. U.S. Environmental Protection Agency (EPA), Report EPA/600/8-90/057F.

Anon., 2006-05-18. Federal Register, MSHA, 71(96): 28928.

ANSYS Inc., 2009. ANSYS FLUENT (12.0) User's Guide.

Kahn G, Orris P, 1988. Acute overexposure to diesel exhaust: report of 13 cases. *J. Am. J. Ind. Med.*, 13(3): 405–406.

Rundell B, Ledin M C, Hammarström U, Stjernberg N, Lundbäck B, Sandström T, 1996. Effects on symptoms and lung function in humans experimentally exposed to diesel exhaust. *Occupational and Environmental Medicine.* 53: 658–662.

Wade J F III, Newman L S, 1993. Diesel asthma: reactive airways disease following overexposure to locomotive exhaust. *Journal of Occupational Medicine*, 35: 149–154.

Zheng Y, Tien J C, 2009a. Simulation of methane distribution at longwall face. In: 2009 SME Annual Meeting. Denver, 1–8.

Zheng Y, Tien J C, 2009b. Reconstruction of diesel emissions distribution based on an isolated zone experiment by using CFD method. In: Proceedings of the 9th International Mine Ventilation Congress. New Delhi, 869–878.